

Calcium isotope fractionation by osteoblasts and osteoclasts, across endothelial and epithelial cell barriers and with binding to proteins

Eva Teresa Toepfer, Jeremy Rott, Maria Bartosova, Ana Kolevica, Irma Machuca, Alexander Heuser, Michael Rabe, Rukshana Shroff, Justine Bacchetta, Sotirios Zarogiannis, et al.

▶ **To cite this version:**

Eva Teresa Toepfer, Jeremy Rott, Maria Bartosova, Ana Kolevica, Irma Machuca, et al.. Calcium isotope fractionation by osteoblasts and osteoclasts, across endothelial and epithelial cell barriers and with binding to proteins. AJP - Regulatory, Integrative and Comparative Physiology, 2021, 321 (1), pp.R29-R40. 10.1152/ajpregu.00334.2020 . hal-03414624

HAL Id: hal-03414624
https://cnrs.hal.science/hal-03414624

Submitted on 4 Nov 2021

HAL is a multi-disciplinary open access archive for the deposit and dissemination of scientific research documents, whether they are published or not. The documents may come from teaching and research institutions in France or abroad, or from public or private research centers.

L'archive ouverte pluridisciplinaire **HAL**, est destinée au dépôt et à la diffusion de documents scientifiques de niveau recherche, publiés ou non, émanant des établissements d'enseignement et de recherche français ou étrangers, des laboratoires publics ou privés.

Type: Original article

Calcium isotope fractionation by osteoblasts and osteoclasts, across endothelial and epithelial cell barriers and with binding to proteins

Eva Teresa Toepfer*, Jeremy Rott*, Maria Bartosova, Michael Rabe,

Kiel: Colleagues next to Toni ?!?

Lyon: Irma Gayet Justine Bacchetta

Rukshana Shroff, Sotiris Zarogiannis, Anton Eisenhauer, Claus Peter Schmitt

1 Centre for Pediatric and Adolescent Medicine, Neuenheimer Feld 430, 69120 Heidelberg, Germany

2 GEOMAR, Helmholtz Zentrum für Ozeanforschung Kiel, 24148 Kiel, Germany

3 Lyon

Corresponding author

Abstract

Timely and accurate diagnosis of osteoporosis is essential for adequate therapy. Calcium isotope ratio determination (δ44/42) in blood and urine has been suggested as a sensitive, non-invasive and radiation-free biomarker for the diagnosis of osteoporosis, reflecting bone calcium balance. The quantitative diagnostic is based on the exact calculation of the δ44/42 calcium difference between blood and bone. The underlying cellular processes, however, have not systematically been studied yet.

We quantified δ44/42 calcium fractionation during in vitro bone formation and resorption by osteoblasts and osteoclast and across confluent renal proximal tubular epithelial cell (RPTEC), endothelial cell (HUVEC) and enterocyte (Caco-2) monolayer in transwell systems, and deterined their transepithelial electrical resistance characteristics. δ44/42 fractionation was furthermore quantified with binding of calcium to albumin and collagen.

Newly formed bone by osteoblast is isotopically lighter than culture medium by -0.27±0.03 ‰ within 5 days, while bone resorption in ur experiemental setting had a small, opposite effect on δ44/42 only. Calcium transport and δ44/42 fractionation also occurs across RPTEC and HUVEC barriers, but not across Caco-2 enterocytes, and not with binding of calcium to albumin and collagen.

On a bone cell level δ44/42 fractionation follows similar principles as during inorganic mineral precipitation; osteoblast activity results in major δ44/42 fractionation. δ44/42 fractionation across renal epithelial cell barriers needs to be considered during bone mineralization modelling, depending on the net calcium fluxes occurring in vivo, whereas the effect of calcium trasnport across endothelial and enteroctye barriers on δ44/42 should be low and absent with physiochemical binding of calcium to proteins.

1. Introduction

In humans, bone mineral balance (BMB) is positive during childhood and adolescence, and supposed to be in an equilibrium of formation and resorption during the so called “peak bone” interval during the age of about 25 to 30 years, and thus the calcium input via the diet and output via sweat, feces and urine [1]. Imbalances, e.g. a net loss of calcium from bone, occurs either after the “peak bone” interval or when pathological changes occur. Imbalances are mostly related to distinct organ or hormonal alterations and diseases, of which osteoporosis is most prevalent, affecting 75 million people in Europe, Japan and the US [2] [3]. In western countries the lifetime risk of an osteoporotic bone fractue is 40-50% in women and 13-22% in men [4], leading to a high economic burden as well as physical and psychological impairment [5] [6]. A sensitive and quantitative determination of BMB is crucial for prevention and early treatment of osteoporosis. The dual x-ray absorptiometry (DXA) is considered the gold standard and measures bone mineral density (BMD) but does provide information on BMB [7]. Biochemical markers such as bone-specific alkaline phosphatase, NTX, P1NP, CTX only qualitatively reflect bone formation or bone resorption but do not provide a measurement of net BMB [5] [8]. Bone biopsies to determine the mineralization status of the bone are invasive and infrequently performed [8-10].In contrast, natural occurring Ca isotopes (CaI) measured in blood serum and urine have been shown to be a potential biomarker for the quantification of mineralization and demineralization processes in the human body [11-15] and may even serve as a sensitive diagnostic tool for the early prediction of osteoporosis [13] [16].

Natural CaI fractionation follows the principle of kinetic isotope fractionation that describes the separation of stable isotopes from each other as a function of their mass during unidirectional biochemical processes [17] [18]. As a consequence of kinetic isotope fractionation, in a chain of chemical reactions the lighter isotope always becomes enriched in the product [16]. In the food chain, lighter isotopes become enriched from plants, via animals to humans [19]. This is quantitatively expressed by decreasing $^{44}Ca/^{42}Ca$ ratios (reported as $\delta^{44/42}Ca$) from vegetables via meat to humans, with the human skeleton as endmember and most enriched reservoir for light CaI [xx]. Kinetic isotope fractionation between diet and skeleton can be applied for diagnostic purposes in order to identify distinct BMB disorders. The principle idea is that the CaI composition of the blood (or urine) is mainly supplied from different sources, the gastro-intestinal tract, the kidneys and the bones of which all contributions have different CaI compositions. In particular any change of the contribution of bone Ca influences the CaI composition of blood to a large extend because it is the isotopically lightest $\delta^{44/42}$ Ca ratio contribution to the blood. In case of decreased bone mineralization as in osteoporosis, a relative increase of light isotopes from the bone can be noted in the blood [16]. In contrast, a high $\delta^{44/42}Ca$ value relative to a threshold value in the blood indicates a net absorption of Ca and bone mass accumulation, as it is the case in children and young adults before reaching the

“peak bone” interval. These basic principles have been verified in bed rest studies [11] [13] and other clinical studies [16] [20] distinguishing healthy and osteoporotic post-menopausal women based on their CaI composition in blood and urine.

For the application of δ44/42 calcium as a diagnostic tool, it is crucial that there is a sufficient isotope difference between blood and bones with the bones having a CaI composition distinctively lower than the blood [21]. Different laboratories have quantitatively confirmed that the CaI fractionation ($\Delta^{44/42}Ca_{Blood\text{-}Bone} = \delta^{44/42}Ca_{Bone} - \delta^{44/42}Ca_{Blood}$) is fairly constant in the order of about $\Delta^{44/42}Ca_{Blood\text{-}Bone} = -0.3$ ‰ and that this value seems to be a universal constant in different species including corals [22] and vertebrates, e.g. chickens, horses [21] and “Göttingen” mini-pigs [23].

However, there is still a lack of information on the cellular level, i.e. whether the $\Delta^{44/42}Ca_{Blood\text{-}Bone}$-value is influenced by osteoblast activity causing δ44/42 fractionation during actively integrating Ca into the organic bone matrix of collagen type 1 or by the opposite effect of bone resorption by osteoclasts, which is expected to be a less active process [24]. Further potential fractionating steps during in vivo Ca transport might be given as Ca is transported across the intestinal barrier, across the vascular endothelium, and across the tubular system of the kidney. Aditionally it is not clear whether and to what extent Ca is fractionated in binding processes such as atomic bonds, ionic bonds or coordinative bonds. In theory a high activation energy enables light isotopes to bind more easily than heavy isotopes; the temporal and physical separation of the CaIs increases. As 80% of bound Ca in the blood is being transported bound to albumin [25] and Ca is bound to collagen in the bone, both binding processes were exmined concerning their fractionation potential.

2. Methods

2.1 Cell culture

2.1.1 Osteoblasts

UMR 106 cells (American Type Culture Collection ATCC, Manassas, VA, USA) were cultured in DMEM (Dulbecco's Modified Eagle Medium, Sigma Aldrich, St. Louis, Missouri, USA) supplemented with 10% FBS (Fetal Bovine Serum, Biochrom GmbH, Berlin, Germany) and 1% Penicillin/Streptomycin, 10000 U/ml (Biochrom GmbH, Berlin, Germany). For passaging the cells were washed with DPBS (Dulbecco's Phosphate Buffered Saline, Gibco; Thermo Fisher Scientific, Inc., Waltham, MA, USA), incubated for 5-10 minutes with Trypsin/EDTA 0.25%/0.02% (Biochrom GmbH, Berlin, Germany) for detachment, centrifuged for 5min at 1000 rounds per minute (rpm, Hettich Universal, RF30) and resuspended in prewarmed medium.

2.1.2 Primary Osteoclasts

Monocytes were purified from peripheral blood of healthy, voluntary consenting donors as previously described [26] [27]. The cells were cultivated in α-minimum essential medium (α -MEM, Gibco; Thermo Fisher Scientific, Inc., Waltham, MA, USA) supplemented with 2mM Glutamin (Gibco; Thermo Fisher Scientific, Inc., Waltham, MA, USA), 1% Penicillin/Streptomycin, 10000 U/ml (Gibco; Thermo Fisher Scientific, Inc., Waltham, MA, USA) , 10% FBS (Merck, Darmstadt, Germany), 40ng/ml human RANKL (PeproTech, Cranbury, NJ, USA) and 20ng/ml human macrophage colony stimulating factor (M-CSF, PeproTech, Cranbury, NJ, USA). For subcultering the cells were washed with DBPS (Gibco; Thermo Fisher Scientific, Inc., Waltham, MA, USA) after 5 days, incubated with 1,5 ml/well Accutase (Sigma Aldrich, St. Louis, Missouri, USA) and centrifuged at 1500 rpm (Thermo Scientific, Heraeus Multifuge X1R) for 10 minutes at 20°C.

2.1.3 Renal proximal tubular cells

Renal proximal tubular epithelial cells (RPTEC; ATCC, Manassas, VA, USA) were cultured in RPMI medium (Thermo Fisher Scientific, Inc., Waltham, MA, USA) with 10% FBS (Biochrom GmbH, Berlin, Germany) and 1% Penicillin/Streptomycin, 10000 U/ml (Biochrom GmbH, Berlin, Germany). Subculturing was executed as described in 2.1.1. All cells were between Passage 10 and 14 at the beginning of the experiment.

2.1.4 Endothelial cells

Human umbilical vein endothelial cells (HUVEC; PromoCell, Heidelberg, Germany) were cultured in Endothelial Cell Growth Medium (PromoCell, Heidelberg, Germany) supplemented with Endothelial Cell Growth Medium Supplement Mix (PromoCell, Heidelberg, Germany) and 1%

Penicillin/Streptomycin, 10000 U/ml (Biochrom GmbH, Berlin, Germany). Cells were subcultured as in 2.1.1 and centifuged at 2000 rmp (Hettich Univeral, 30RF). All cells were between Passage 5 and 9 at the beginning of the experiment.

2.1.5 Enterocytes

Caco-2 cells (ATCC, Manassas, VA, USA) were cultured in high Glucose DMEM (Sigma Aldrich, St. Louis, Missouri, USA) with 1% non-essential aminoacids (Sigma Aldrich, St. Louis, Missouri, USA), 10% FBS (Biochrom GmbH, Berlin, Germany) and 1% Penicillin/Streptomycin, 10000 U/ml (Biochrom GmbH, Berlin, Germany). Cells were subcultured by using 5 ml Accutase (Sigma Aldrich, St. Louis, Missouri, USA) for 7 minutes of incubation, the remaining subculture steps were according to 2.1.1. All cells were at Passage 12 at the beginning of the experiment.

2.2 Bone formation

UMR 106 cells were harvested and seeded in six-well plates at a density of 1×10^5 cells per well. At 80% confluency, the growth medium (DMEM) was replaced by Osteoblast Mineralization Medium (PromoCell, Heidelberg, Germany) and cells were cultured for 5 days. The negative control received the standard growth medium (DMEM). Samples were taken at 0, 12, 24, 72 and 120 hours and centrifugated for 5min at 1000 rpm (Hettich Universal, RF30).

For the detection of Ca deposits, the staining solution was prepared dissolving Alizarin Red S (Carl Roth GmbH + Co. KG, Karlsruhe) in distilled water and pH was adjusted to 4.2. After washing the cells with PBS (Sigma Aldrich, St. Louis, Missouri, USA), the cellular monolayer was fixed with 10% neutral buffered formalin (Sigma Aldrich, St. Louis, Missouri, USA) for 30 min. Next, the fixed solution was removed and the cells were washed with distilled water. Finally, the staining solution was added and remained for 45min, before washing the cells again with distilled water.

2.2 Bone resorption

Detached human Osteoclasts obtained after 5 days of standard culture were planted on an Osteo Assay Surface 24 well plate (Corning Incorporated, Corning, NY, US) at a density of $1x10^5$ cells/well dissolved in 700µl medium per well ~~and cultured for 5 days~~. From this timepoint on the α-MEM was supplemented with 2mM Glutamin, 1% Penicillin/Streptomycin, 5% FBS and 10ng/ml M-CSF. Half of the dwells were supplemented with 40ng/ml RANKL (RANKL+).

Tartrate-resistant acid phosphatase (TRAP, Sigma Aldrich, St. Louis, Missouri, USA) and silver nitrate (Merck, Darmstadt, Germany) stainings were performed after 24, 48 and 72 hours according to the manufacturer's manual.

For determination of intracellular calcium RANKL+ and RANKL- cells were planted on Osteo Assay Surface 24 well plate and on sterile 24 well plastic cell culture plates (Falcon; Corning Incorporated, Corning, NY, US) at a density of 1,3 x 10^5 cells/well in a volume Jaof 1000µl/well. After 24h the cells were lifted with Accutase, centrifuged as described above and resuspended in 300µl serum free α-MEM Medium.

2.3 Transwell Experiments

Transwells (Costar, 6,5mm Inserts, 24 well Plate, 0,4µm polyester membrane, Corning Incorporated, Corning, NY, US) were primed with cell culture medium for two hours before 5x10^4/well renal proximal tubular cells and endothelial cells and 4x10^4 enterocytes were seeded per well. The basolateral compartment was filled with 1500µl of the respective culture medium, the apical compartment contained 300 µl of culture medium with a two- fold higher calcium, achieved by Ca-chloride-dihydrate dissolution (J.T. Baker Phillipsburg, NJ, USA). Transepithelial electrical resistance (TER) was measured with MILLICELL-ERS and the experiment was started, when TER reached a stable plateau [28].

Experiments on the calcium and CaI transport over 8 hours, were followed by experiments investigating the short-term transport kinetics over 32 minutes. Each calcium and CaI determination equaled a separate transwell insert.

2.5 Albumin and collagen binding

Ca gluconate 10% (B. Braun, Melsungen, Germany) was chosen as Ca donor and diluted in a ratio of 1:100 (original concentration 230 mmol/l) with 0.9% NaCl solution (B. Braun, Melsungen, Germany). The Ca stock solution (2.3 mmol/l) was incubated with increasing albumin concentrations (0, 2.5, 5 and 10 g/l albumin; Serva Electrophoresis GmbH, Heidelberg, Germany) over 24h at 37°C, 5%CO_2 and constant humidity. The lid was sealed with paraffin foil. For each experiment culture wells were filled with 1000µl solution, of which 500µl were filtered before determinations. Filtration was performed with a 10kDa centrifugal filter (Merck, Darmstadt, Germany) at 11500 rpm (Eppendorf 5417 R) for 20 minutes to remove albumin and the bound Ca.

Calcium binding to collagen was measured using 0, 20 and 40 µg/ml human collagen type 1 (Merck, Darmstadt, Germany). 500µl solution were used, of which 250 µl underwent the same filtration process as for the albumin studies after 0, 12 and 24 hours of incubation.

2.6 Protein quantification

Collagen samples as described in 2.5 were incubated for 0, 12 and 24 hours in a concentration of 40, 80 and 160µg/ml. A positive control with 200µg/ml collagen was added. 25µl of each collagen sample

was diluted with 4x loading buffer (containing 4% ß-mercaptoethanol). Proteins were separated in a 10% polyacrylamide gel at 200 V for 45 min. The protein transfer onto a polyvinylidenfluoride (PVDF) membrane was performed in a Transblot Cell (Bio-Rad Laboratories, Munich, Germany) at 105 V for 90 min. Afterwards the membrane was blocked with blocking buffer (3% bovine serum albumin and 5% milk) for 2 hours at room temperature on a shaker followed by an overnight incubation with COL1A1 antibody, 1:200 (Cell Signaling Technology, Danvers, MA, USA) at 4°C. Then the membrane was washed three times for 5, 10 and 15 min with 0.05% Tris-buffered saline with Tween20 (TBS-T). The membrane was then incubated for one hour with secondary antibody (anti rabbit IgG conjugated to horseradish peroxidase, 1:3000, Cell Signaling Technology, Danvers, MA, USA) at room temperature, followed by three washing steps (?) with 0.05% TBS-T. After adding detection reagents (GE Healthcare, Buckinghamshire, UK) the collagen samples were quantified densitometrically using Image Lab Software (Bio-Rad, USA).

2.7 Chemical sample preparation and mass-spectrometry measurements of total calcium concetrations and calcium isotopes

All samples were stored at -20°C immediately after sample collection and transported on dry ice. The chemical sample preparation (sample digestion and purification) as well as the mass spectrometer set up were performed as previously described [29]. In bone formation and resorption experiments calcium concentration and CaI ratios were determined in culture media and in the synthetic bone layer. For the latter, the bone matrixes were dissolved in 1000 µl HNO_3 2M/well. Of each plate consisting of 24 bone matrix wells one was used for initial calcium and CaI determination, ruling out manufactural differences.

2.8 Quantification of bone resorption

To quantify the resorption of primary osteoclasts the wells of the Osteo Assay Surface plate were scanned at 2x magnification (ACQUIFER Imaging Machine), merged by Fiji tool for batch stitching [30] and analyzed using ImageJ software. To this end pictures were changed into a binary mode; the sum of white pixels corresponding to resorption pits was presented as percentage of total pixel count.

2.9 Statistical Analysis

At least three independent experiments were performed with osteoblasts, primary osteoclasts and albumin binding experiments. Two independent experiments were conducted concerning calcium collagen binding as well as two independent short- and long-term experiments with enterocytes and endothelial cells and one short and one long-term experiment was performed with endothelial cells. For statistical analysis Graph Pad Prism 8 (La Jolla, CA, USA) was used. Descriptive data were

summarized using means and standard deviation (SD). To assess the differences between groups ANOVA or student´s t-test were used. In all cases two sided tests were performed and $p < 0.05$ was considered statistically significant.

3. Results

3.1 Bone formation

UMR106 osteoblasts were cultured for 5 days with and without ossification inducing medium. The medium calcium concentration of non-actived osteoblasts increased by 0,3±0.16 mmol/L within 5 days (Fig. 3A), due to medium evaporation to 20.3±1.8% of the initial volume. In contrast, the medium calcium concentration of activated osteoblasts decreased by 0.6±0.2 mmol/l together with continuous in vitro bone formation. The calcium concentration of the synthesized deposits increased from 0.2 mmol/L after 12 hours to 1.9 mmol/L after 120 hours.

The CaI ratio in the medium of inactivated osteoblasts ($\delta^{44/42}Ca_{control}$) did not change (Fig. 1 B), whereas the medium CaI ratio of activated osteoblasts ($\delta^{44/42}Ca_{activated}$) steadily increased to 0.12±0.03‰ above baseline within 5 days. In line with this, the CaI ratio of the mineralized deposits ($\delta^{44/42}Ca_{deposit}$) decreased from 0.18±0.05‰ to a minimum of 0.10±0.02‰ within 72 hours. This resulted in CaI difference between deposits and medium ($\Delta_{deposit\ -\ activated} = \delta^{44/42}Ca_{deposit} - \delta^{44/42}Ca_{activated}$) of -0.27±0.03 ‰ after 5 days. From a simple mass balance equation, the relative partitioning "f" of the original CaI in the culture medium of activated osteoblasts can be calculated from equation 1:

(1) $$\delta^{44/42}Ca_{control} = f \cdot \delta^{44/42}Ca_{activated} + (1-f) \cdot \delta^{44/42}Ca_{deposit}\ ; 0 \leq f \leq 1$$

The term f can be calculated to be 0.66 which is interpreted to reflect the amount of Ca remaining in the solution after 120 hours whereas about 34% corresponding to about 6.8%/day of the Ca originally present in the solution was precipitated.

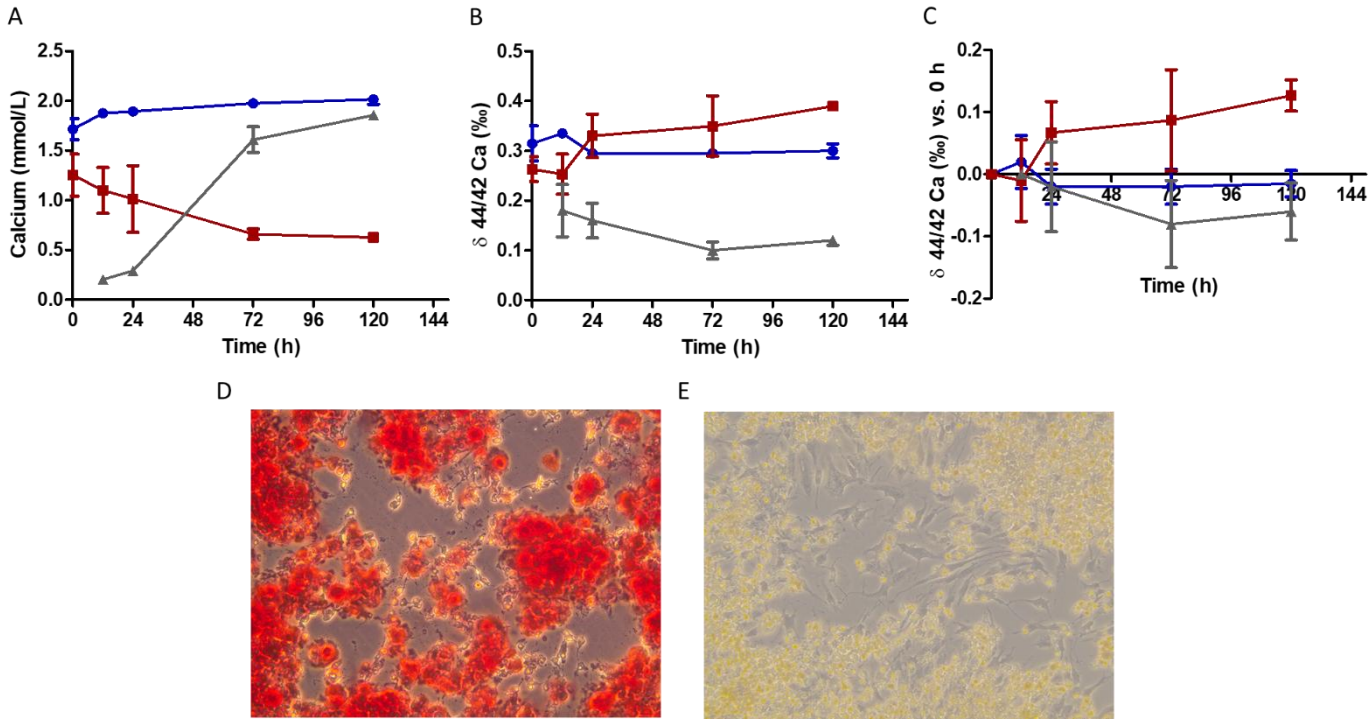


Fig. 1 Calcium and CaI kinetics with bone formation
Changes in medium calcium concentrations with activated (red squares) and inactivated UMR106 cells (blue circles) and of the re-dissolved mineralized deposits generated by the activated UMR106 cells (grey triangles) are given in (A). The respective changes in absolute CaI ratios over time (δ44/42 calcium) are given in (B), δ44/42 calcium changes relative to baseline values in (C) and representative calcium deposit stainings (Alizarin red) of activated and inactivated osteoblasts in (D) and (E).

3.2 Bone resorption

RANKL supplementation resulted in differentiation from monocytes to active osteoclasts, since these were TRAP positive, multinucleated and exerted bone resorbing activity (Fig. 2 A, C, E). After 72h RANKL activated primary osteoclasts had absorbed 2.52 % of the bone matrix, inactivated osteoclasts 0.71% (Fig. 2 E).

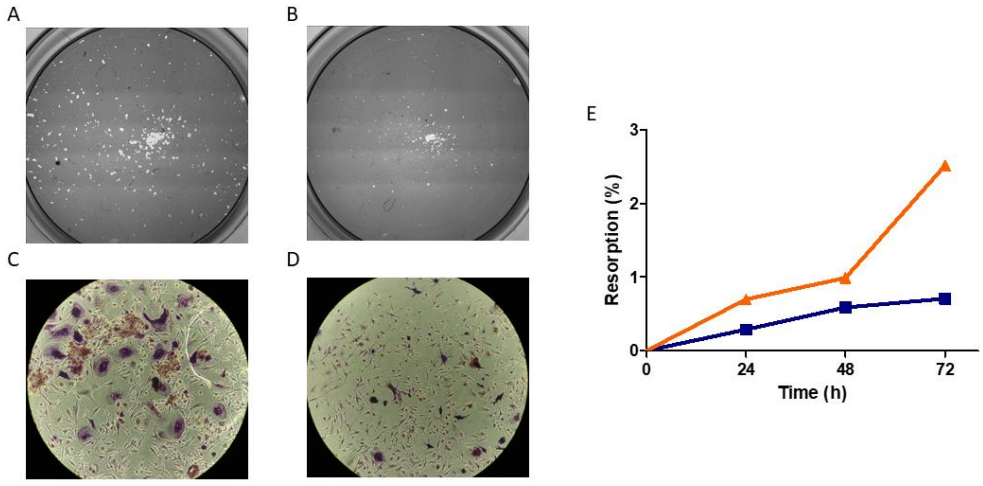


Fig. 2 Bone matrix resorption by osteoclasts

Silver nitrate staining of bone matrix after 72h of incubation with A) RANKL activated and B) non-activated primary osteoclasts (magnification 2-fold). TRAP staining of (C) activated and (D) inactivated osteoclast (magnification 20-fold). Quantification of silver nitrate stained bone resorption pits by RANKL activated (orange triangles) and non-activated primary osteoclasts (blue squares) is given in (E).

Due to the pre-treatment of monocytes with RANKL some, small osteoclasts were also present in cultures not stimulated with RANKL during the experiment. CaI ratio increased with incubation time in both groups ($p<0.002/0.0001$ RANKL neg/pos; 72h versus baseline), more so, however, in cultures with continuously RANKL stimulated cells (two-way repeated ANOVA, $p=0.08$). At 72h, the delta in $\delta^{44/42}$Ca was 0.078±0.015‰ in RANKL activated and 0.045±0.013‰ in RANKL-inactivated osteoclasts (t-test, $p=0.017$; $n=4$) (Figure 3 A, B).

The medium calcium concentration, however, did not change with activated and inactivated osteoclasts (Fig. 3 C). Evaporation of the culture medium over 72 h amounted to 11.8±3.4 %, which should have contributed to an increase in medium calcium concentration of 1.76± 0.04 mmol/l at baseline by 0.21±0.01 mmol/l. Calcium removal by RANKL activated osteoclasts from the artificial bone matrix after 72h was calculated. The Ca content of the entire bone matrix dissolved in 1 ml HNO3 was 0.63±0.05 mmol/L. According to the equation:

(0.63 mmol/l x 2.5 % resorption area * 10^{-3} L) / (0,0007 L culture medium volume)

the increase in medium concentration by bone resorption of activated osteoclasts should be 0.023 mmol/l. Thus, total increase in medium calcium should have amounted to 0.23 mmol/l. Since medium calcium concentrations did not increase with medium evaporation and osteolysis (Fig.3 C); calcium precipitation must have occurred. In line with this, the calcium concentration of the bone matrix (Fig 3 D) increased with time by 0.27±0.04 mmol/l as did the $\delta^{44/42}$ calcium of the bone matrix (+0.10±0.03 ‰; Figure 3 E). The latter is explained by the low $\delta^{44/42}$ calcium of the bone matrix relative to the internal standard and the high $\delta^{44/42}$ calcium of the culture medium (0.36±0.01 ‰). Intracellular calcium concentrations and the cellular distribution volume are low, major cell lysis did not occur. Therefore, these do not contribute significantly to the calcium kinetics. Intracellular calcium concentration and the $\delta^{44/42}$ of the cellular calcium was higher in RANKL activated osteoclasts (Fig. 3 F).

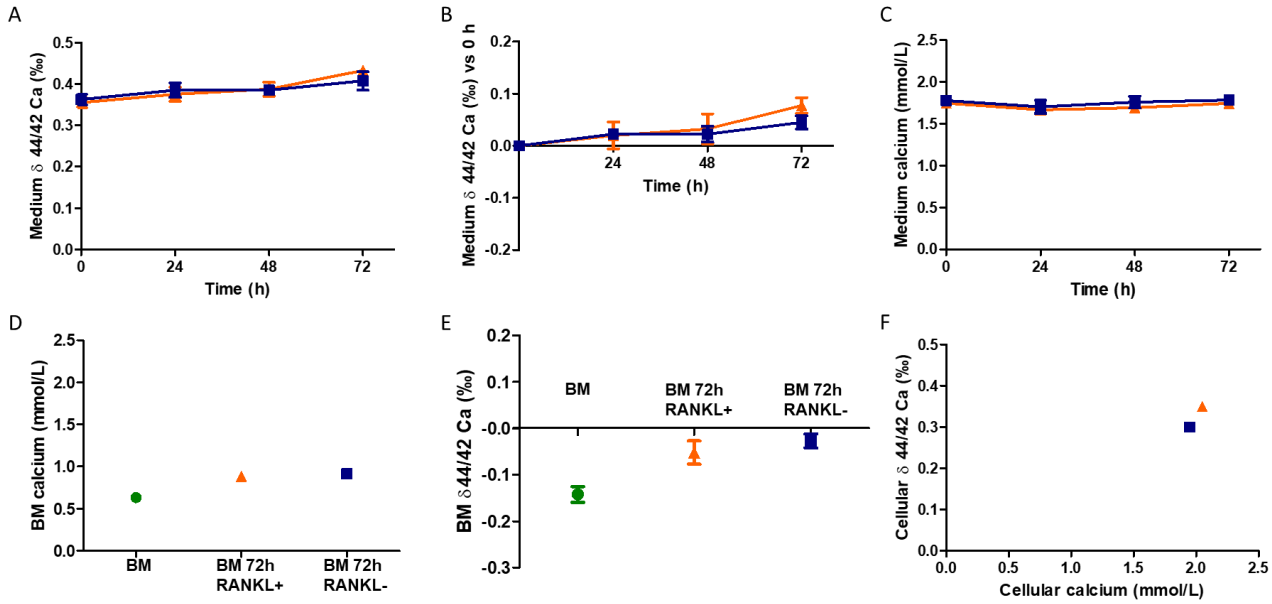


Fig. 3: Calcium and CaI kinetics with resorption of the bone matrix
The absolute calcium δ44/42 calcium ratios (A) and relate to baseline (B) are given over 72 h of incubation with RANKL activated (orange triangles) and non-activated primary osteoclasts (blue squares). Medium calcium concentrations (C), however, remained unchanged. Calcium precipitation occurred; since calcium content of the unused bone matrix (BM; green circle; BM dissolved in 1 ml of HNO3) was lower than the calcium content of the BM after 72h of incubation with activated and non-activated osteoclasts (D). The calcium isotope ratio of the BM relative to the internal standard also increased with precipitation (E), due to the higher medium δ44/42 calcium ratio as compared to the original BM. (F) gives the intracellular calcium concentration and the δ44/42 calcium ratio of osteoclasts after 24 hours of incubation on BM with and without RANKL stimulation. For the latter osteoclasts of 6 RANKL positive and 6 RANKL negative cultures were pooled and intracellular calcium concentrations and δ44/42 calcium ratios measured.

3.3 Calcium transport and isotope fractionation across endothelial and tubular epithelial cells and enterocytes

3.3.1 Transepithelial electrical resistance

To characterize the barrier function of epithelial and endothelial cell monolayers TER was repeatedly measured until confluency and TER reached a plateau (supplemental figure 1). At this time point calcium transport measurements were performed. While RPTEC proximal tubular cells and endothelial cells reached confluency and a stable and relatively low TER within 3 days, enterocytes required about 5 times longer but reached a very high TER (Table 3).

Table 3: Transepithelial electrical resistance (TER) of cell and incubation time in transwell systems until TER reached the plateau phase. RPTEC = Renal proximal tubular epithelial cells, HUVEC =Human Umbilical Endothelial Cells, Cacao2 = Enterocytes

Cell line	TER (Ω/cm^2)	Incubation time (days)

HUVEC	13.3	3
RPTEC	17.2	3
Caco-2	2228	15

3.3.2. Calcium- and CaI-kinetics

To induce calcium transport across the cell barriers the apical compartment contained higher calcium concentrations than the basolateral one, depending on the physiological culture needs of the respective cells. In HUVEC the initial gradient was 1.27 ± 0.01 mmol/l, in RPTEC 0.78 ± 0.16 mmol/l and in Caco-2 1.48±0.08 mmol/l. The calcium concentration steadily declined in the apical compartment and increased in the basolateral with HUVEC, reaching similar values, i.e. an equilibrium of about 1.85 mmol/l after 8h. The decline in calcium in the apical compartment and the increase in the basolateral compartment were less pronounced with RPTEC reaching - 0.36 ± 0.02 mmol/l and +0.03 ± 0.03 mmol/l after 8h, respectively. In Caco-2 the calcium concentration declined in the apical compartment by -0.48 ± 0.26 mmol/l, and remained largely unchanged in the basolateral compartment over 8 h (Figure 4 A, E, I). In HUVEC transwell cultures the δ44/42 increased during the first hour in the apical compartment and slightly declined in the basolateral, while minor changes were observed with RPTEC and Caco-2 monolayers (Fig. 4 B, F, J). Beyond 2 hours all three cell types maintained a gradient of the δ44/42 calcium ratio until 8 hours.

To better understand the initial transport kinetics, transwell experiments were performed over 32 min. Similar trends in calcium concentrations changes in apical and basolateral compartments were observed with the three different cell types as shown over 8h, but the C δ44/42 calcium kinetics differed substantially. In RPTEC transwell cultures the δ44/42 calcium transiently increased in the apical compartment within 16 min by 0.26 ‰, and in HUVEC within 8 min by 0.13 ‰. This was followed by an equilibration of the CaI ratios between the apical and basolateral compartment with both cell types. In Caco-2 the δ44/42 calcium remained again unchanged (Fig. 4D, H, L). The short term RPTEC transwell experiment was repeated with a lower initial calcium gradient between the compartments of 0.21 mmol/l. A similar, transient increase in δ44/42 calcium in the apical compartment of 0.32 ‰ was observed (supplemental figure 2).

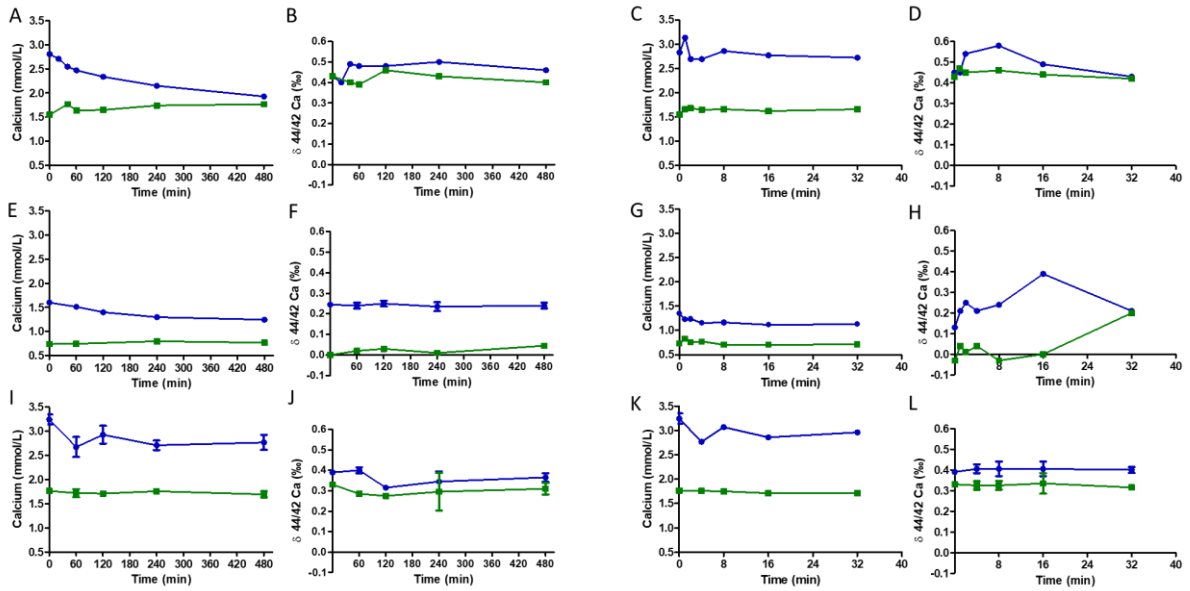


Fig. 4: Calcium- and δ44/42 calcium kinetics across endothelial and tubular epithelial cells, and enterocytes. Calcium and δ44/42 calcium kinetics over 8 hours (two graphs on the left) and over 32 minutes (two graphs on the right side) are depicted for HUVEC (first line), RPTEC, (second line) and Caco-2 (lower line). δ44/42 calcium fractionation occurs with HUVEC during the first 8 min, and more pronounced with RPTEC during the first 16 min, but not with Caco-2 cells. The volume of the culture medium is 300 µl in the apical (blue line) and 1500 µl in the basolateral compartment (green line).

3.4 Binding experiments

3.3.1 Calcium binding to albumin and collagen

To study the effect of calcium binding to albumin on δ44/42 calcium, medium was supplemented with increasing doses of human albumin and incubated for 3 and 24 h, followed by filtration of the medium to remove the albumin and bound calcium. After 3 and 24 hours, calcium concentrations had declined with increasing albumin concentrations, i.e. increase albumin binding, but the δ44/42 calcium remained unchanged (Fig 5 A, B).

Similar results were obtained with calcium binding to collagen over 24 h. While the calcium concentration declined with increasing collagen concentrations, the δ44/42 calcium remained unchanged (Fig 5 C, D). Of note, different form the albumin experiment, the calcium concentration also declined in the unfiltered solutions, because most of the collagen was bound to the well, as illustrated by the western blot (Fig 5E).

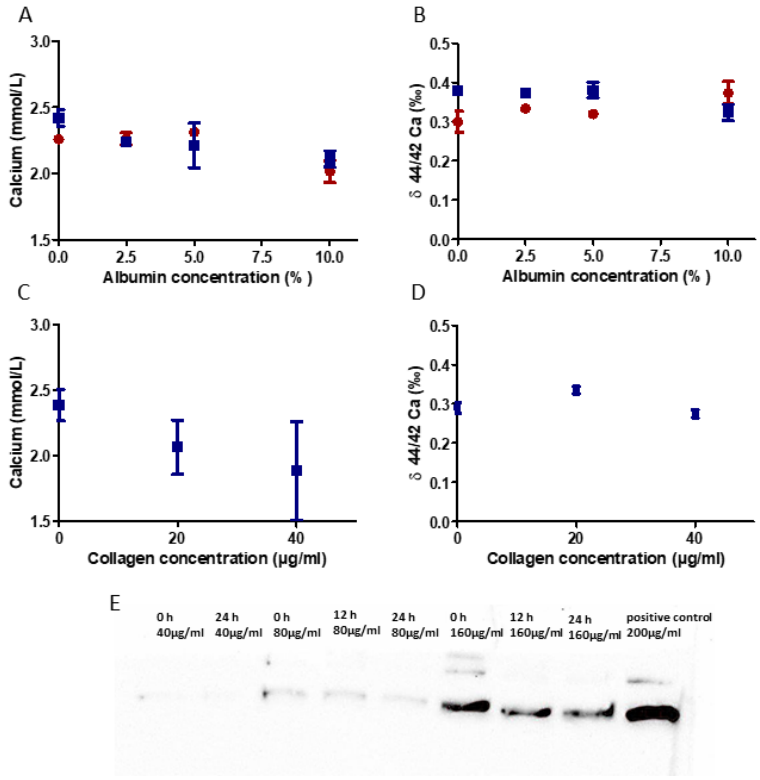


Fig. 5: Calcium concentration and δ44/42 calcium after incubation with albumin for 3 h (red circle) and 24 h (blue square) (A,B) and after 24 h of incubation with collagen (C,D). While the calcium concentration declined with increasing albumin and collagen concentrations, the δ44/42 calcium in the solution remained unchanged. Whereas albumin had to be filtered out of the solution to remove the calcium bound to albumin, collagen and the bound calcium were attached to the well surface, as illustrated by western blotting (E).

4 Discussion

Bone diseases are highly prevalent, but diagnosis is hampered by the limited information provided by imaging techniques and blood biomarkers. Both do not provide information on the mineralization process of bone. Bone quality, however, essentially depends on adequate mineralization, i.e. on the calcium turnover [31]. Blood and urine CaI ratios (δ44/42 calcium) have been suggested as a sensitive marker of the bone mineralization process [13] [16] [20]. We now provide essential information on the contribution of bone and epithelial and endothelial cells to the δ44/42 calcium fractionation process. Bone matrix formation by osteoblasts results in a preferential deposition of lighter isotopes, while osteoclasts remove slightly more heavy isotopes from the bone matrix. Lighter CaI are preferentially transported across the leaky epithelial cell barriers formed by RPTEC and by HUVEC, while no significant δ44/42 calcium fractionation occurred across Caco-2 enterocytes and with binding of calcium to albumin and collagen.

Bone contains 10% water, 30-40% proteins and 50-60% inorganic components, namely hydroxyapatite crystals [32] Mineralization requires a series of physicochemical and biochemical processes that facilitate the deposition of calcium phosphate, subsequently converted into hydroxyapatite. Osteoblasts synthesize organic bone matrix proteins, mainly collagen, and release matrix vesicles which contain the biochemical machinery needed for the mineralization process [33]. The matrix vesicles bind to the collagenous matrix via specific proteins and lipids and following vesicle break the collagenous matrix is exposed to the hydroxyapatite [33]. CaI fractionation occurs during crystallization processes e.g. during volcanic eruptions [34] and during coral calcification in concert with endosymbiotic flagellates (ref). …. (Toni please elaborate as appropriate!). We now demonstrate that within this process of bone mineralization by osteoblasts δ44/42 calcium fractionation takes place, the lighter isotope is preferentially deposited. Thus, osteoblasts contribute to the δ44/42 calcium gradient between blood and bone in vivo ($\Delta^{44/42}Ca_{Blood\text{-}Bone}$) as reported in various species [21-23]. These findings confirm that this value is produced by inorganic mineral precipitation alone and that no additional chemical processes must be involved.

Osteoclasts form closed areas on the calcified bone matrix, and actively secrete H^+ and proteases into these lacunae for dissolution of the hydroxyapatite bone matrix at a pH of 4-4.5. The products are endocytosed, and transcytosed to specific release domains at the contralateral area of the plasma membrane, where they are released into the interstitial space [35]. To study whether fractionation of δ44/42 calcium occurs with osteolysis, in a first approach, we studied RANKL activated RAW 264.7 cells. These, however, did not dissolve quantifiable amounts of bone matrix, even not with concomitant LPS and TNF-alpha incubation over up to 21 days (data not shown). We therefore used human primary osteoblasts, which time dependently dissolved up to 2.5% of the bone matrix within 3 days. Accounting for daily medium evaporation, release of calcium from the bone matrix by osteoclasts, calcium precipitation on the bone plate and osteoclast cell lysis with release of minor quantities of intracellular calcium we were able to analyse calcium shifts and δ44/42 calcium changes. Pre-stimulated and during the experiment unstimulated osteoclasts exerted less osteolysis than the continuously stimulated osteoclasts, but both resulted in a slight increase in medium δ44/42 of calcium; more so in the activated osteoclasts. The underlying mechanisms are uncertain, but neither explained by evaporation nor by precipitation, because both processes are not energy consuming, and therefore have no fractionation potential. Whether crystallization favoring lighter isotopes occurred following the precipitation of calcium on the artificial bone matrix (which contains organic matrix), or whether the osteoclasts preferentially removed heavy isotopes from the bone plate cannot be discerned. The slightly higher intracellular calcium concentration and the higher δ44/42 calcium in activated versus non-activated osteoclasts argues in favor of the latter. In vivo, the δ44/42 calcium fractionation process may be modified by interactions of the different cell types and under the control of circulating factors such as vitamin D and PTH.

Osteocytes are a promising therapeutic target to improve bone health, since they essentially orchestrate bone remodeling by regulating osteoclast and osteoblast activity, and thus bone loss and formation [36]. Since they do not directly act on the bone mineralization we did not study their effect on δ44/42 calcium fractionation.

Next to the impact of bone cells on circulating δ44/42 Ca we studied the impact of epithelial and endothelial cell barriers. The calcium gradient continuously declined in HUVEC, but not in the other cell lines, where after an initial adaptation phase a calcium gradient was maintained across the cell layer for up to 8h. δ44/42 calcium fractionation occurred during the first few minutes after establishing the calcium gradient. Lighter CaI were preferentially transported across RPTEC, and to a smaller extend also across HUVEC monolayers, while no significant δ44/42 Ca fractionation occurred across Caco-2. These findings have to evaluated in view of the physiological cell functions. Unbound calcium, i.e. 55% of total plasma calcium is freely filtered across the glomerular barrier; a large amount of calcium, of which 60-70 are reabsorbed in the proximal tubule. The majority of this

calcium reabsorption occurs via a passive, paracellular process driven by active solute and subsequent water reabsorption [37]. In this unidirectional process, which under physiological conditions never reaches a steady state [38], lighter calcium isotopes should be transported faster. We now demonstrate that this is the case; δ44/42 calcium fraction across the PRPTEC, the lighter isotopes are preferentially transported. This finding is in line with data from patients with chronic kidney disease and ….

The amount of calcium transport across endothelial cells in vivo is much smaller as compared to that across RPTEC and depends on the vessel site. It is bidirectional, i.e. transendothelail calcium uptake occurs e.g. in the intestine and loss occurs e.g. into an anabolic bone, using the transcellular and the paracellular route (ref). The observed δ44/42 calcium fractionation was smaller and should quantitively contribute less to δ44/42 calcium measured in blood.

Caco-2 enterocytes formed a tight barrier in vitro, as reflected by the very high transepithelial resistance, calcium transport should mainly occur via the transcellular route, involving … In vivo both routes are active. In case, the intestinal luminal calcium concentrations exceed the plasma concentrations, the paracellular pathway is predominantly used, in case they are lower, calcium is actively absorbed via the transcellular pathway, mainly in the duodenum [39] [40]. Our in vitro studies using the colorectal tumor derived Caco-2 cell line reflects the former condition.

Our studies have several limitations. Since δ44/42 calcium determinations require laborious and costly analyses: The experiments had to be limited to one to two per setting, but where underpinned by sufficient data density. Key findings such as the marked δ44/42 calcium fractionation across RPTEC were repeated in a similar setting. In the transwell experiments, the δ44/42 calcium of the calcium stock solution supplemented to the different cell culture mediums used, therefore the initial δ44/42 calcium gradient in the transwells varied between different cell types. An impact on the δ44/42 calcium fractionation process is unlikely but not excluded. The in vitro setting does not reflect the complex network of modifying factors of calcium transport and bone mineralization. Still, we provide yet unknown insight into the principles of δ44/42 calcium fractionation in the bone and across renal proximal tubular epithelial cell system, across endothelial cells and tight enterocytes, and the presumed relative contribution to blood, urine and bone δ44/42 calcium isotope distribution measured in vivo. Physiochemcal binding of calcium to proteins such as albumin and collagen does not modify δ44/42 calcium ratio.

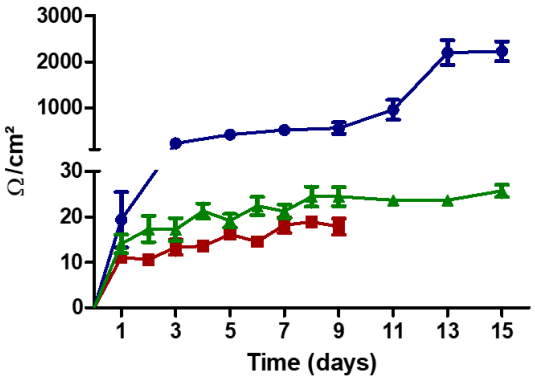
Acknowledgements

…... are acknowledged for ….. We thank Martin Schneider, Dept of Surgery, Heidelberg, for providing the Caco2 cells. We thank M. Zorn for technical assistance.

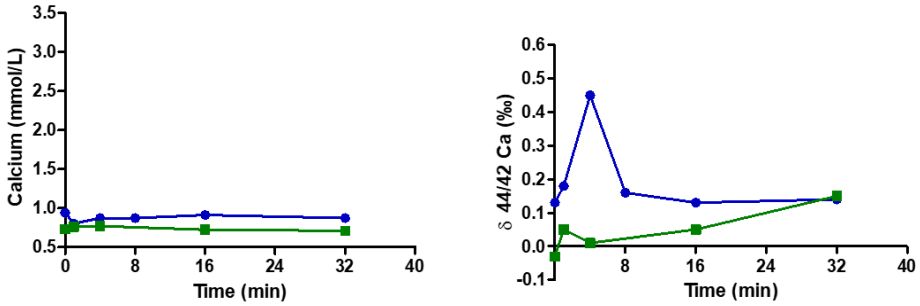
Funding

MB is funded by the Deutsche Forschungsgemeinschaft (DFG, German Research Foundation) – Projektnummer 419826430. SGZ acknowledges the Alexander von Humboldt Stiftung/Foundation for an Experienced Researcher Fellowship (2019-2021) and the International Peritoneal Dialysis Society (ISPD) for an International Cooperation Research Grant (2019-2021). CPS received a research grant from AMGEN and has obtained funding from European Nephrology and Dialysis Institute (ENDI).

Supplemental figures



Suppl. Fig. 1: Transepithelial electrical resistance (TER, Ω/cm²) of HUVEC (red squares), RPTEC (green triangles) and Caco-2 cells (blue circles) over time of culture, until cell confluency and a steady state level of TER was reached.



Suppl. Fig. 2: Short-term calcium and *δ44/42 calcium kinetics across renal proximal tubular epithelial cells. Calcium concentration are given on the left graph, δ44/42 calcium on the right graph. The initial medium calcium gradient between apical (blue line; volume 300 µl) and basolateral compartment (green line; volume 1500 µl) was 0.21 mmol/l. A marked increase in δ44/42 calcium occurred in the apical compartment within 4 mins.*

References

1. Bartl, R.B., C, *Bone Disorders: Biology, Diagnosis, Prevention, Therapy* 2017: Springer International Publishing Switzerland.
2. Johnell, O. and J.A. Kanis, *An estimate of the worldwide prevalence, mortality and disability associated with hip fracture.* Osteoporos Int, 2004. **15**(11): p. 897-902.
3. *Who are candidates for prevention and treatment for osteoporosis?* Osteoporos Int, 1997. **7**(1): p. 1-6.
4. Johnell, O. and J. Kanis, *Epidemiology of osteoporotic fractures.* Osteoporosis International, 2005. **16**(2): p. S3-S7.
5. Lane, N.E., *Epidemiology, etiology, and diagnosis of osteoporosis.* Am J Obstet Gynecol, 2006. **194**(2 Suppl): p. S3-11.
6. Svedbom, A., et al., *Balloon kyphoplasty compared to vertebroplasty and nonsurgical management in patients hospitalised with acute osteoporotic vertebral compression fracture: a UK cost-effectiveness analysis.* Osteoporos Int, 2013. **24**(1): p. 355-67.
7. Kanis, J.A., *Diagnosis of osteoporosis and assessment of fracture risk.* Lancet, 2002. **359**(9321): p. 1929-36.
8. Lalayiannis, A.D., et al., *Assessing bone mineralisation in children with chronic kidney disease: what clinical and research tools are available?* Pediatr Nephrol, 2019.
9. Barreto, F.C., et al., *Bone biopsy in nephrology practice.* J Bras Nefrol, 2018. **40**(4): p. 366-374.
10. Evenepoel, P., et al., *Update on the role of bone biopsy in the management of patients with CKD-MBD.* J Nephrol, 2017. **30**(5): p. 645-652.
11. Channon, M.B., et al., *Using natural, stable calcium isotopes of human blood to detect and monitor changes in bone mineral balance.* Bone, 2015. **77**: p. 69-74.
12. Gordon, G.W., et al., *Predicting multiple myeloma disease activity by analyzing natural calcium isotopic composition.* Leukemia, 2014. **28**(10): p. 2112-2115.
13. Morgan, J.L.L., et al., *Rapidly assessing changes in bone mineral balance using natural stable calcium isotopes.* Proceedings of the National Academy of Sciences of the United States of America, 2012. **109**(25): p. 9989-9994.
14. Rangarajan, R., et al., *Assessing bone mineral changes in response to vitamin D supplementation using natural variability in stable isotopes of Calcium in Urine.* Sci Rep, 2018. **8**(1): p. 16751.
15. Skulan, J., et al., *Natural calcium isotopic composition of urine as a marker of bone mineral balance.* Clin Chem, 2007. **53**(6): p. 1155-8.
16. Eisenhauer, A., et al., *Calcium isotope ratios in blood and urine: A new biomarker for the diagnosis of osteoporosis.* Bone reports, 2019. **10**: p. 100200-100200.
17. Bullen, T.D. and A. Eisenhauer, *Metal Stable Isotopes in Low-Temperature Systems: A Primer.* Elements, 2009. **5**(6): p. 349–352.
18. Eisenhauer, A., B.a. Kisakürek, and F. Böhm, *Marine Calcification: An Alkali Earth Metal Isotope Perspective.* Elements, 2019. **5**(6): p. 365-368.
19. Chu, N.-C., et al., *Establishing the potential of Ca isotopes as proxy for consumption of dairy products.* Applied Geochemistry, 2006. **21**(10): p. 1656-1667.
20. Heuser, A. and A. Eisenhauer, *A pilot study on the use of natural calcium isotope (44Ca/40Ca) fractionation in urine as a proxy for the human body calcium balance.* Bone, 2010. **46**(4): p. 889-96.
21. Skulan, J. and D.J. DePaolo, *Calcium isotope fractionation between soft and mineralized tissues as a monitor of calcium use in vertebrates.* Proc Natl Acad Sci U S A, 1999. **96**(24): p. 13709-13.
22. Böhm, F., et al., *Calcium isotope fractionation in modern scleractinian corals.* Geochimica et Cosmochimica Acta, 2006. **70**(17): p. 4452-4462.
23. Heuser, A., et al., *Biological fractionation of stable Ca isotopes in Gottingen minipigs as a physiological model for Ca homeostasis in humans.* Isotopes Environ Health Stud, 2016. **52**(6): p. 633-48.
24. Yamaki, M., et al., *Transcytosis of calcium from bone by osteoclast-like cells evidenced by direct visualization of calcium in cells.* Arch Biochem Biophys, 2005. **440**(1): p. 10-7.

25. Besarab, A. and J.F. Caro, *Increased absolute calcium binding to albumin in hypoalbuminaemia.* Journal of clinical pathology, 1981. **34**(12): p. 1368-1374.
26. Fugier-Vivier, I., et al., *Measles virus suppresses cell-mediated immunity by interfering with the survival and functions of dendritic and T cells.* The Journal of experimental medicine, 1997. **186**(6): p. 813-823.
27. Allard, L., et al., *Biphasic Effects of Vitamin D and FGF23 on Human Osteoclast Biology.* Calcif Tissue Int, 2015. **97**(1): p. 69-79.
28. Ghaffarian, R. and S. Muro, *Models and methods to evaluate transport of drug delivery systems across cellular barriers.* Journal of visualized experiments : JoVE, 2013(80): p. e50638-e50638.
29. Morgan, J.L., et al., *High-precision measurement of variations in calcium isotope ratios in urine by multiple collector inductively coupled plasma mass spectrometry.* Anal Chem, 2011. **83**(18): p. 6956-62.
30. Gehrig, J., *Fiji tool for batch stitching of ACQUIFER Imaging Machine data*, in *http://doi.org/10.5281/zenodo.3631724*, Zenodo, Editor. 2020, January 30.
31. Clarke, B., *Normal bone anatomy and physiology.* Clin J Am Soc Nephrol, 2008. **3 Suppl 3**(Suppl 3): p. S131-9.
32. Feng, X., *Chemical and Biochemical Basis of Cell-Bone Matrix Interaction in Health and Disease.* Current chemical biology, 2009. **3**(2): p. 189-196.
33. Bolean, M., et al., *Biophysical aspects of biomineralization.* Biophys Rev, 2017. **9**(5): p. 747-760.
34. Antonelli, M.A., et al., *Ca isotopes record rapid crystal growth in volcanic and subvolcanic systems.* Proc Natl Acad Sci U S A, 2019. **116**(41): p. 20315-20321.
35. Florencio-Silva, R., et al., *Biology of Bone Tissue: Structure, Function, and Factors That Influence Bone Cells.* BioMed research international, 2015. **2015**: p. 421746-421746.
36. Kitaura, H., et al., *Osteocyte-Related Cytokines Regulate Osteoclast Formation and Bone Resorption.* Int J Mol Sci, 2020. **21**(14).
37. van der Wijst, J., et al., *Learning Physiology From Inherited Kidney Disorders.* Physiol Rev, 2019. **99**(3): p. 1575-1653.
38. Edwards, A., *Regulation of calcium reabsorption along the rat nephron: a modeling study.* American Journal of Physiology-Renal Physiology, 2015. **308**(6): p. F553-F566.
39. Bronner, F., *Calcium absorption--a paradigm for mineral absorption.* J Nutr, 1998. **128**(5): p. 917-20.
40. Gloux, A., et al., *Candidate genes of the transcellular and paracellular calcium absorption pathways in the small intestine of laying hens.* Poult Sci, 2019. **98**(11): p. 6005-6018.